Geophysical Research Letters

RESEARCH LETTER
10.1029/2019GL084786

Climatology Explains Intermodel Spread in Tropical Upper Tropospheric Cloud and Relative Humidity Response to Greenhouse Warming

Stephen Po-Chedley[1], Mark D. Zelinka[1], Nadir Jeevanjee[2,3], Tyler J. Thorsen[4], and Benjamin D. Santer[1]

[1]Program for Climate Model Diagnosis and Intercomparison (PCMDI), Lawrence Livermore National Laboratory, Livermore, CA, USA, [2]Department of Geosciences, Princeton University, Princeton, NJ, USA, [3]Geophysical Fluid Dynamics Laboratory, Princeton, NJ, USA, [4]NASA Langley Research Center, Hampton, VA, USA

Key Points:
- Tropical upper tropospheric clouds and relative humidity in climate models track isotherms, which rise in response to greenhouse warming
- Intermodel differences in cloud and relative humidity changes are related to model climatology, which shifts up with CO_2-mediated warming
- Observations provide a constraint on simulated changes in tropical upper tropospheric clouds and relative humidity

Supporting Information:
- Supporting Information S1

Correspondence to:
S. Po-Chedley,
pochedley1@llnl.gov

Citation:
Po-Chedley, S., Zelinka, M. D., Jeevanjee, N., Thorsen, T. J., & Santer, B. D. (2019). Climatology explains intermodel spread in tropical upper tropospheric cloud and relative humidity response to greenhouse warming. *Geophysical Research Letters*, *46*. https://doi.org/10.1029/2019GL084786

Received 31 JUL 2019
Accepted 30 SEP 2019
Accepted article online 17 OCT 2019

Abstract The response of upper tropospheric clouds and relative humidity (RH) to warming is important to the overall sensitivity of the Earth to increasing greenhouse gas concentrations. Previous research has shown that changes in hydrologic fields should closely track rising isotherms in a warming climate. Here we show that the distribution of tropical clouds and RH in general circulation models is approximately constant under greenhouse warming when using temperature as a vertical coordinate. By assuming that these fields are an invariant function of atmospheric temperature and that temperature change follows a dilute moist adiabat, we are able to accurately predict cloud fraction and RH changes in the tropical upper troposphere (150–400 hPa) in 27 general circulation models. Our results indicate that intermodel spread in changes of tropical upper tropospheric clouds and RH is closely related to differences in model climatology and could be substantially reduced if model ensembles reliably reproduced observed climatologies.

Plain Language Summary As the Earth warms due to increasing greenhouse gas concentrations, many aspects of the climate adjust. Clouds, for example, tend to shift upward in response to surface warming. Such processes, known as climate feedbacks, alter the radiative energy that reaches the Earth's surface and, as a result, can amplify or damp global warming. One method for investigating climate feedbacks is to analyze their behavior in global climate models. Because clouds and relative humidity exhibit widely varying responses to warming in climate models, uncertainty in the Earth's sensitivity to changes in atmospheric carbon dioxide is exacerbated. Building on previous theoretical research, we demonstrate that the simulated response of clouds and relative humidity to global warming is closely associated with model representation of the present-day climate. Theory, observations, and climate models indicate that moistening of the troposphere and rising of the highest cloud tops cause large positive feedbacks. Our research suggests that the substantial model spread in representing these feedbacks may be reduced by improving simulations of the observed present-day climate.

1. Introduction

The response of clouds and humidity to warming is an important contributor to the Earth system's sensitivity to greenhouse gas (GHG) concentration changes (Caldwell et al., 2016; Charney et al., 1979; Hansen et al., 1984). The moistening that accompanies atmospheric warming decreases outgoing radiation, resulting in a large, positive climate feedback. Warming also produces higher cloud tops, which diminishes outgoing longwave radiation because the cloud top emission temperature declines with increasing altitude (Hartmann & Larson, 2002). This cloud altitude feedback is positive in both the tropics and extratropics, increasing the Earth's sensitivity to GHG concentration changes (Zelinka et al., 2016).

The basic response of the atmosphere to GHG concentration changes is to warm and moisten at nearly constant relative humidity (RH; Manabe & Wetherald, 1975). The radiative effect of such moistening is the water vapor feedback, which is a function of the vertical structure of atmospheric warming (Soden & Held, 2006). Since the structure of atmospheric temperature change is largely driven by the meridional pattern of surface warming, both the lapse rate and water vapor feedback are closely tied to the spatial pattern of surface

warming (Po-Chedley et al., 2018; Soden & Held, 2006). Although the atmosphere generally moistens at near-constant RH, changes in RH are nonnegligible, particularly in the tropics (O'Gorman & Muller, 2010; Vial et al., 2013). Tropical RH changes result in a decoupling between the tropical lapse rate and water vapor feedbacks and drive the spread in the tropical water vapor feedback across general circulation models (GCMs; Po-Chedley et al., 2018; Vial et al., 2013). On a global scale, RH changes account for roughly half of the intermodel spread in the total water vapor feedback, and the sign of the RH feedback is not known (Held & Shell, 2012). Changes in RH are similar to the response of cloud fraction to warming in GCMs, which frequently use RH in their parameterization of cloud fraction (Sherwood et al., 2010; Wetherald & Manabe, 1980).

The changes in RH and clouds that result from greenhouse warming have considerable spread across GCMs. A substantial body of research offers insights into the causes of such model differences. Hartmann and Larson (2002) identified basic thermodynamic and radiative processes that constrain high tropical anvil clouds to a fixed temperature. This is frequently referred to as the Fixed Anvil Temperature (FAT) hypothesis, which is supported by observations, GCM simulations, and cloud-resolving models (Eitzen et al., 2009; Harrop & Hartmann, 2012; Kubar et al., 2007; Kuang & Hartmann, 2007; Xu et al., 2007; Zelinka & Hartmann, 2010, 2011). Since isotherms rise as the troposphere warms, high clouds are expected to rise in order to maintain constant temperature. Recent work suggests that the FAT hypothesis also applies to the extratropics (Thompson et al., 2017, 2019). Although it is well-documented that increasing cloud altitude with warming results in a positive radiative feedback (Zelinka & Hartmann, 2010), the magnitude of this feedback is not well constrained (Zelinka et al., 2016).

Motivated by studies demonstrating that geophysical fields exhibit an upward shift as the planet warms (e.g., Lorenz & DeWeaver, 2007; Mitchell & Ingram, 1992; Santer et al., 2003), Singh and O'Gorman (2012) investigated the changes in clouds, RH, mass stream function, and temperature in simulations performed under Phase 3 of the Coupled Model Intercomparison Project (CMIP3). For these fields, they found that a relatively simple vertical transformation of the model climatology captures the key features of the zonal mean response to GHG warming. Consistent with the FAT hypothesis, their vertical shift was formulated to closely match the rise in isotherms with warming. Sherwood et al. (2010) demonstrated that, across CMIP3 GCMs, the response of RH in the tropical and extratropical upper troposphere scales with the climatological vertical gradient of RH, which indicates that model climatology is important to simulated changes in RH. In an analytical model of tropical RH, Romps (2014) found that tropical RH should be an invariant function of temperature in the free troposphere. This was demonstrated to be a reasonable approximation in atmospheric GCM simulations with prescribed sea surface temperatures (SSTs; Jeevanjee & Romps, 2018, their Figure S11).

Collectively, this research indicates that temperature is expected to be a dominant control on upper tropospheric clouds and RH, particularly in the tropics. In this paper, we analyze simulations performed under phase 5 of CMIP (CMIP5) and confirm that in the tropics, these hydrologic fields track rising isotherms in response to greenhouse warming. Previous research demonstrated that the rise of isotherms should closely follow a moist adiabat in the tropics (Santer et al., 2005). Under this assumption, we show that the tropical RH and cloud response to GHG warming in CMIP5 models can be accurately predicted.

2. Data Sets and Methods

2.1. General Circulation Model Data

In order to investigate differences in the cloud and RH response to greenhouse warming across GCMs, we employ climate models that participated in CMIP5 (supporting information Table S1; Taylor et al., 2012). We use two pairs of experiments.

We first consider the historical and RCP8.5 simulations performed with 27 different CMIP5 models (Table S1). Since the historical simulations end in 2005, we extend them with data from the RCP8.5 simulations through 2018 to create 39-year climatologies (1980–2018) of cloud fraction, RH, and air temperature. The time series were inspected to ensure there are no discontinuities between the historical and RCP8.5 simulations. We select the 1980 to 2018 time period to facilitate comparison with current reanalysis products (see below). To estimate the model response to combined anthropogenic forcing by well-mixed GHGs, stratospheric ozone, and aerosols, the 39-year GCM climatologies are compared to climatologies derived

from the last 39 years of the 21st century (averaged over 2061 to 2099 in RCP8.5). Selecting shorter time periods had little impact on our results.

Observations of cloud fraction are not directly comparable to standard model cloud fraction fields. Models represent clouds in horizontally and vertically coarse atmospheric layers. In contrast, observations of cloud properties have widely varying spatiotemporal sampling and are not always able to detect all clouds in a vertical column. These differences need to be accounted for before comparing model cloud fraction with observational cloud products. To facilitate this comparison, we use a "model-to-satellite" approach. GCM fields are used to estimate what a satellite-based instrument would observe if it were sampling the model atmosphere (Bodas-Salcedo et al., 2011; Chepfer et al., 2008). We use output from a lidar simulator embedded in GCMs that is intended to emulate the cloud occurrence seen by the Cloud-Aerosol Lidar and Infrared Pathfinder Satellite Observation (CALIPSO) system (Winker et al., 2009). This allows us to compare the synthetic cloud lidar data from GCMs to the real-world CALIPSO observations (discussed below).

Although cloud fraction is available from all 27 models, only two models have cloud lidar output from both the historical and RCP8.5 experiments. To maximize the number of models considered, we use data from the Atmospheric Model Intercomparison Project (AMIP), in which the observed SST is prescribed as a boundary condition (eight models; see Table S1). For this experiment, we utilize the last 10 years (1999–2008), which is the same length as the observed CALIPSO cloud record discussed below. To evaluate the model response to surface warming, we use the AMIP4K experiment, which has the same specifications as AMIP, but with a uniform 4 K increase in SST. Model temperature data from the AMIP simulations is regridded from pressure levels to altitude levels (corresponding to the cloud lidar simulator grid) using the hypsometric equation.

GCM output is regridded to a 1.5° × 1.5° grid and standard pressure levels, though we leave the model cloud lidar data on the native altitude grid. Since the troposphere deepens with warming, we also calculate the height of the lapse rate tropopause, which is determined from model temperature data using a standard World Meteorological Organization definition (Reichler et al., 2003). All model data analyzed here is available for download from the Earth System Grid Federation.

2.2. Observations and Reanalyses

We compare model RH climatologies with data from two reanalysis products: the Modern-Era Retrospective analysis for Research and Applications, Version 2 (MERRA2; Gelaro et al., 2017) and the Fifth Generation of European Centre for Medium-Range Weather Forecasts reanalysis (ERA5; Copernicus Climate Change Service (C3S), 2017). For simplicity, we refer to these reanalysis products as observations, even though atmospheric reanalysis involves use of an atmospheric model to assimilate a variety of different observations. We regrid the reanalysis data to the same 1.5° × 1.5° grid and standard pressure levels used for the GCM data. Both of the reanalysis products are available from 1980–2018, which allows us to compare the reanalysis and GCM data over the same time period.

In addition to reanalysis, we also use humidity observations over 2005–2015 from a combined Atmospheric and Infrared Sounder (AIRS) and Microwave Limb Sounder (MLS) data set (Liang et al., 2010). The AIRS/MLS water vapor concentration data are converted to RH using the temperature data included with the product and then mapped to a 2.5° × 2.5° monthly grid.

We compare the GCM lidar simulated cloud fields with two CALIPSO cloud occurrence products: the GCM-Oriented CALIPSO Cloud Product (GOCCP), which was specifically developed for comparisons with climate models (Chepfer et al., 2010) and the National Aeronautics and Space Administration (NASA) CALIPSO Lidar Level 3 Cloud Occurrence Standard Monthly Product v1.00. We consider 10 full years of CALIPSO data from both data sets (2007 through 2016). The observed temperature climatology is also used in our analysis; this field comes from the temperature observations embedded in the NASA CALIPSO Level 3 Product (which are subsetted from MERRA2).

The two reanalyses and the observed AIRS/MLS product provide a measure of the structural uncertainty across RH data sets, which is useful given that substantial differences exist between MLS RH observations and atmospheric reanalyses (Jiang et al., 2015). Similarly, differences between the GOCCP and NASA CALIPSO data sets capture structural uncertainty in these retrievals. Although the reanalysis products span the last 39 years, the CALIPSO and AIRS/MLS time series are relatively short. Furthermore, since the AMIP simulations end in 2008, the model period has little overlap with real-world CALIPSO observations, which began in June 2006. When we analyze nonoverlapping 2-year time periods from the model simulations

(within 1999–2008), each period yields consistent results for both RH and cloud occurrence, which indicates that complete overlap is not critical to this analysis. As for the model data, we calculate the tropopause height using the temperature fields from each observational and reanalysis data set.

2.3. Methods

Our main objective is to estimate the expected cloud fraction and RH change in response to anthropogenic forcing under the assumption that their vertical distribution is dictated by temperature. In each column and for each month, we assume that the cloud fraction and RH profiles are simply a function of temperature, $C(T)$, where C represents the climatological cloud amount or RH within a vertical column and T is the temperature profile of the free troposphere (the stratosphere is excluded from our analysis). With knowledge of the future temperature profile (with respect to pressure, p) in response to anthropogenic forcing, $T'(p)$, we can then estimate the future profile of clouds and RH, $C'(p)$. We estimate the future temperature profile using the assumption that warming follows a dilute moist adiabat (Romps, 2016; see Figure S1). A moist adiabat assumes that ascent in convective plumes is undiluted. In reality, entrainment of dry air dilutes the updraft and modifies the lapse rate.

We use a dilute moist adiabat because it better represents key features of the simulated tropical atmospheric temperature climatology and change (Figures S2a and S2b). While both the conventional moist adiabat and dilute moist adiabat overestimate the ratio of atmospheric to surface warming in the tropical upper troposphere, this bias is smaller in the latter case (Figure S2c).

Although extratropical upper tropospheric warming is tightly connected to tropical surface warming in simulations with GHG increases, the magnitude of extratropical upper tropospheric warming is overestimated using both a dilute and undilute moist adiabat (Po-Chedley et al., 2018). Furthermore, most research that connects the distribution of clouds and RH to temperature is specific to the tropical atmosphere. For these reasons, we focus on the tropics. In the tropics, we can reliably estimate the profile of warming using the difference between dilute moist adiabat profiles at 299 (the approximate tropical average SST) and 300 K assuming 80% RH at the surface (as in Flannaghan et al., 2014).

The dilute moist adiabat is calculated by integrating the temperature lapse rate from the surface to the tropopause. This formulation has one free parameter, which we set to approximately match the multimodel average profile of atmospheric temperature change (a = 1.0 in Equation 7 of Romps, 2016). We approximate the future temperature profile in each model column by adding this reference profile of dilute moist adiabatic warming to the temperature climatology. We then estimate the end-of-century distribution of clouds and RH using (1) the climatological relationship between each hydrologic field and temperature and (2) the estimate of future atmospheric temperature. The difference between our prediction of the future state and the climatologies of clouds and RH yields an estimate of the change expected per degree centigrade of surface warming. The expected change in clouds and RH for both models and observations are calculated in each column using the same profile of dilute moist adiabatic warming.

To estimate the prediction uncertainty that arises from interannual variability, we use a subsampling approach. For the reanalysis fields, we use seven nonoverlapping 5-year climatologies and estimate the expected change in RH for each time period. For the CALIPSO cloud fields (NASA and GOCCP data sets), we consider day-only, night-only, and combined day and night climatologies. Since the CALIPSO record is shorter, we subsample five individual 2-year periods, which yields 15 predictions of the tropical cloud response. For AIRS/MLS RH data, we also sample five individual 2-year periods.

3. Results

We begin by considering the historical and RCP8.5 simulations. In the multimodel climatological mean (1980–2018), tropical cloud fraction and RH tend to increase with altitude between 600 and about 150–200 hPa (see black contours in Figures 1a and 1b). Above this height, cloud fraction and RH decrease with altitude. In response to GHG-induced warming, the CMIP5 multimodel mean exhibits a decrease in RH and cloud fraction below ~200 hPa and an increase in these quantities near the tropopause at the end of the 21st century (2061–2099; see shading in Figures 1a and 1b). These simulated responses are consistent with an upward shift of the climatological distribution of clouds and RH. Given that CMIP5 models have varying degrees of sensitivity to GHGs, the changes shown in Figure 1 are normalized by the tropical mean surface air temperature change. The absolute increase in the tropopause height from the multimodel mean

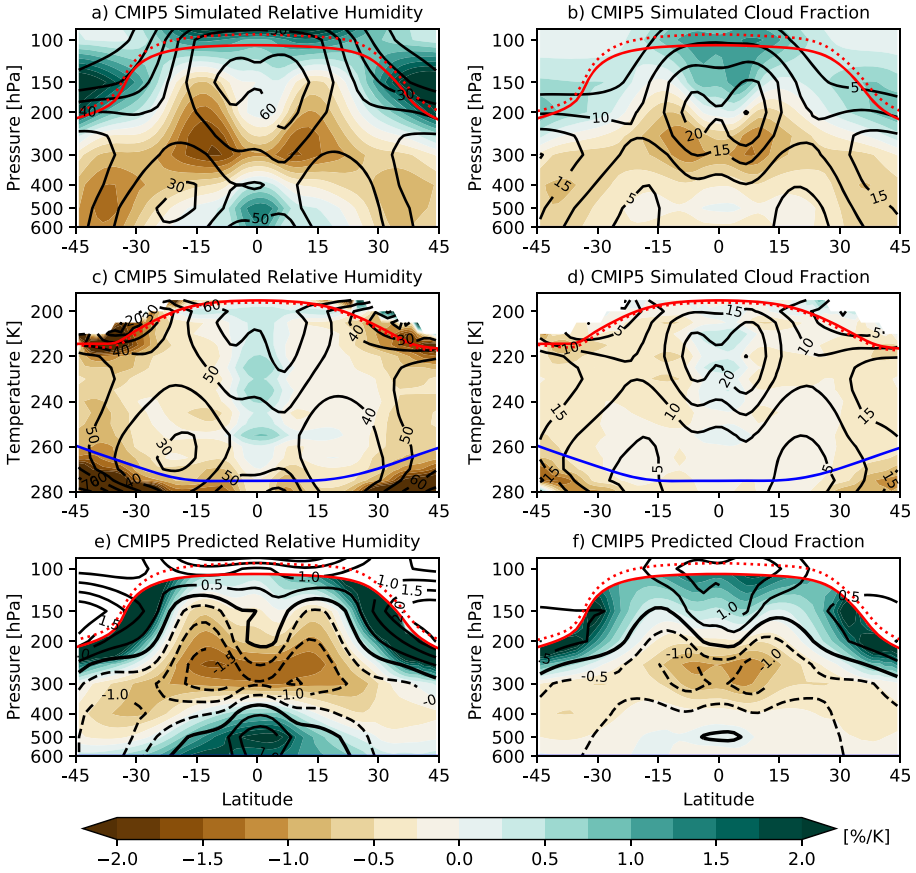

Figure 1. Zonal and annual mean (a) relative humidity (RH) and (b) cloud fraction climatologies (1980–2018 average; contours) and simulated end-of-century change (shading) for the Phase 5 of the Coupled Model Intercomparison Project (CMIP5) multimodel average. The second row is the same but using temperature as a vertical coordinate instead of pressure for (c) RH and (d) cloud fraction. The shading in the third row shows the multimodel average predicted change in (e) RH and (f) cloud fraction in pressure coordinates (the simulated change from panels a and b is contoured on panels e and f for reference). The 600-hPa isobar and tropopause are indicated with solid blue and red lines, respectively. The dashed red line represents the multimodel average tropopause height at the end of the 21st century (2061–2099). Note that the vertical coordinates use a log(pressure) weighting and the area above the tropopause is masked in panels e and f. Changes in RH and cloud fraction are the differences between the recent and end-of-century climatologies and are normalized by the tropical (30° S to 30° N) average surface temperature change.

climatological value to the end-of-century (cf. solid and dashed red lines in Figure 1) yields information on the magnitude of simulated changes in the depth of the troposphere.

Changes in RH, cloud fraction, and tropopause height are much smaller if temperature is used as a vertical coordinate, particularly in the tropics (Figures 1c and 1d). This indicates that changes in these fields tend to track with isotherms as the Earth warms. Some of the changes in clouds and RH (see Figures 1c and 1d) likely result because the multimodel mean hydrologic response is influenced by physical processes other than the vertical shift considered here. For example, a broad barotropic drying poleward of 30° in both hemispheres has been attributed to Hadley Cell expansion (e.g., Lau & Kim, 2015).

We can also use each CMIP5 model's climatology to estimate the expected response of RH and cloud fraction to anthropogenic warming. To estimate this response, we assume that both of these fields are an invariant function of temperature and that the normalized profile of warming can be approximated using a dilute moist adiabat (see section 2 and Figure S1). The multimodel average of each model's predicted response is shaded in Figures 1e and 1f. The results are comparable to those from Singh and O'Gorman (2012), who applied a similar methodology to CMIP3 models. The changes estimated from the CMIP5 model climatologies are similar to the multimodel mean simulated response (black contours in Figures 1e and 1f), with relatively small differences in the pattern and magnitude. For example, the multimodel average predicted

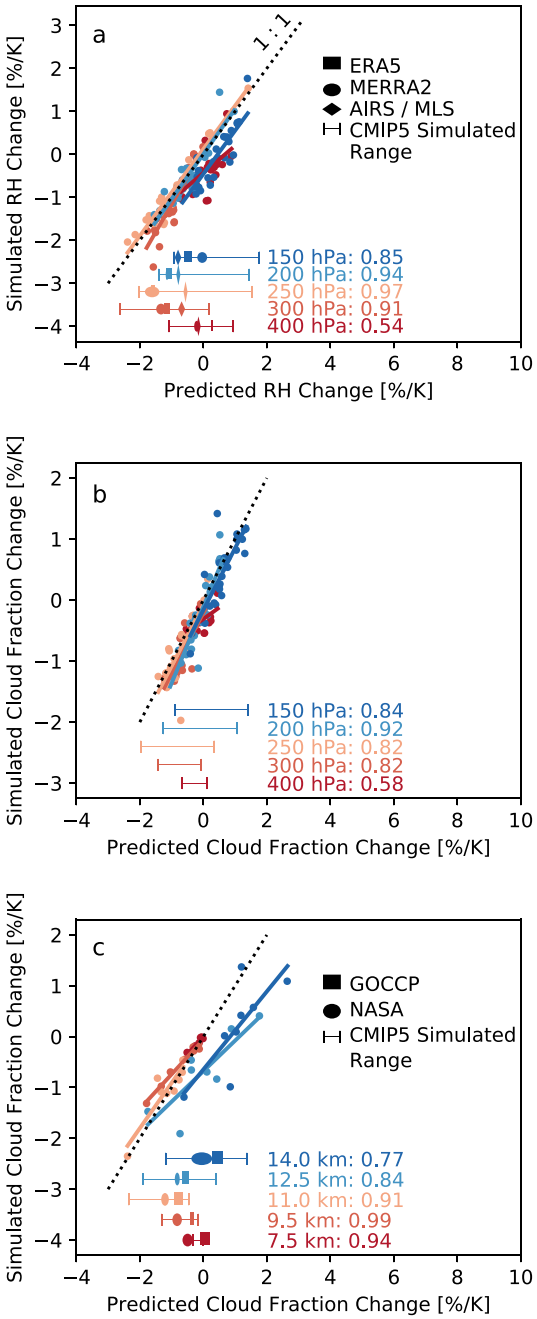

Figure 2. General circulation model simulated tropical (30° S to 30° N) and annual average (a) relative humidity (RH) and (b) cloud fraction change per degree of surface warming versus the changes predicted using each general circulation model's RH and cloud fraction climatology. The results are shown as a function of pressure level (150–400 hPa, colors), and the correlation coefficient is indicated for each level (the slope in each regression is statistically significant at a stipulated significance level of $p < 0.05$). (c) As in panel b but for lidar simulated cloud occurrence at altitude levels that approximately correspond to the pressure levels in panel b. The simulated and predicted changes in each panel are normalized by the tropical average surface warming and tend to fall along the 1:1 line (dotted black line). The predicted change from the observations is also shown with symbols (see legends). The width of the observational markers in panels a and c represents the range of the predictions that results from interannual variability (see section 2). Because we cannot calculate the end-of-century change for the observed fields, the location on the ordinate axis is irrelevant. For context, the total spread in the CMIP5 *simulated* change is indicated with horizontal lines for each level.

response shows enhanced drying (moistening) above the equator near 250 (500) hPa. The predicted pattern also tends to have less meridional structure and exhibits enhanced moistening along the tropopause at roughly 30° in both hemispheres.

Figure 1 displays the multimodel mean hydrologic climatologies and responses to greenhouse warming. This masks substantial intermodel spread in the RH and cloud climatologies and responses (Figures S3 and S4, respectively). Models with small vertical gradients in their cloud and RH climatology have relatively small simulated changes by the end of the 21st century (e.g., FGOALS-g2). The opposite is true of models with large vertical gradients (e.g., GFDL-CM3).

Such qualitative agreement between climatological gradients and hydrologic changes raises the question: Can model differences in climatology reliably predict the intermodel spread in the response of RH and cloud fraction to greenhouse warming? To answer this question, we estimate the expected change in both fields using each model's climatology (assuming an invariant relationship with temperature and that warming follows a dilute moist adiabat). For each model, we compare the climatology-based estimate of the tropical (30° S to 30° N) average change with the actual simulated tropical average change. We focus on the tropics for several reasons: The tropics is where our assumption of dilute moist adiabatic warming is most defensible, previous research motivating our analysis is particularly focused on this region (e.g., Hartmann & Larson, 2002; Romps, 2014), and the tropical domain is where model spread in the radiative response to RH changes is largest (Po-Chedley et al., 2018).

Throughout the tropical upper troposphere (150–400 hPa), the estimated response is a significant predictor ($p < 0.05$) of the actual change for both RH and cloud fraction (Figures 2a and 2b, respectively). The GHG-induced change inferred from the climatological mean state generally captures the magnitude of the simulated change at each level (dashed one-to-one line, Figure 2). Although we have predicted the changes in RH and clouds using the dilute moist adiabat in each column, the results are not substantially different if we instead use each model's actual change in atmospheric temperature (Figures S5a and S5c) or if we use tropical average fields to make our prediction (instead of averaging spatially resolved predictions; see Figure S5b and S5d). Our collective results demonstrate that model simulations of future changes in tropical upper tropospheric clouds and RH are closely related to model representation of the current climate.

Given the accuracy of the climatology-based estimates of RH and cloud fraction changes across CMIP5 models, it is of interest to calculate the expected RH changes derived from the reanalyses and AIRS/MLS climatologies (Figure 2a). At each level, hydrologic changes estimated from these observations are within the range of the model simulated changes (the horizontal lines represent the range of the *simulated* changes across models). Note that because the prediction is imperfect, some model predicted values (dots on the x axis) are outside of the simulated model range (bars). The observations indicate that a strong reduction of RH is expected between 200 and 300 hPa, with little or no reduction of RH at 150 and 400 hPa (Figure 2a; the patterns of the predicted RH changes from the reanalyses and AIRS/MLS data are shown in Figure S3).

While our analysis focuses on the tropics, we can also use climatological means to explain the intermodel spread in RH and cloud fraction changes in the extratropical upper troposphere (Figure S6). To predict the magnitude of extratropical RH and cloud changes, we need a reliable estimate of extratropical tropospheric temperature changes, since a moist adiabat is not applicable outside the tropics. If we use the simulated extratropical atmospheric temperature change in each model and define the extratropics as 45–90° to avoid including the effects of Hadley Cell expansion, the predicted changes in clouds and RH scale with the simulated changes (Figure S7). The predicted changes in extratropical clouds and RH are less accurate relative to the tropics, perhaps due to dynamical changes (e.g., the poleward migration of the midlatitude jet streams). Nevertheless, our results suggest that temperature is an important factor in determining cloud and RH changes in the extratropics.

In addition to the conventional "raw" model cloud fraction field, we also consider the simulated cloud lidar data calculated from the AMIP and AMIP4K experiments. As for the conventional cloud fraction field, there is a strong correlation between the predicted and simulated changes in the synthetic CALIPSO cloud fraction, although the results deviate from the one-to-one line in the tropical upper troposphere (Figure 2c). This deviation is probably partly due to uncertainty in calculating the synthetic CALIPSO cloud occurrence from standard model fields. Our result suggests that use of synthetic cloud observations preserves the relationships between climatological mean state and forced changes found with conventional model cloud output.

As with the AIRS/MLS and reanalysis-based estimates of RH change, the cloud changes inferred from the GOCCP and NASA CALIPSO data sets are consistent with an upward shift in clouds as the planet warms (Figure 2c altitude levels are comparable to the pressure levels in Figure 2a).

We obtain some sense of structural and temporal sampling uncertainty by using multiple data sets (NASA/GOCCP and MERRA2/ERA5) and by creating predictions of future hydrologic change using subsampled climatologies (see section 2.3). The predicted response across all subsampled observational estimates has less spread compared to the CMIP5 intermodel spread at levels above 400 hPa (7.5 km for CALIPSO). On average, the range of the expected response of cloud fraction and RH from observations is 32% of the model range (simple average over 150- to 400-hPa levels in Figures 2a and 2c). There is reasonable agreement across different observational data sets and subsampled time periods. This agreement implies that observations of clouds and RH serve as a useful benchmark for model evaluation and could lead to substantial reductions in the range of simulated changes of tropical upper tropospheric cloud fraction and RH.

4. Discussion

This research was motivated by a number of investigations (including Hartmann & Larson, 2002; Romps, 2014; Sherwood et al., 2010; Singh & O'Gorman, 2012; Zelinka & Hartmann, 2010). Romps (2014) explicitly noted that RH should be an invariant function of temperature in the tropical free troposphere, particularly in regions of deep convection. Given the close correspondence between GCM cloud and RH changes (Figures S3 and S4), it follows that cloud properties should also be closely associated with atmospheric temperature. The association between high clouds and temperature is typically explained using the FAT hypothesis (Hartmann & Larson, 2002), which differs from the analytical framework developed by Romps (2014) for RH. Both studies point toward temperature as a key determinant of the distribution of tropical upper tropospheric clouds and RH.

Recent research using cloud-resolving radiative convective equilibrium experiments with simplified physics has questioned the physical underpinnings of the FAT hypothesis. Seeley et al. (2019) noted that although the tropopause temperature is nearly constant, consistent with our results (Figure 1), their results do not support a constant anvil cloud temperature. Perhaps a better characterization of the "fixed" anvil temperature is that changes in high cloud temperatures are suppressed relative to the surface temperature change, which is evident in a wide range of studies (Harrop & Hartmann, 2012; Hartmann & Larson, 2002; Hartmann et al., 2019; Khairoutdinov & Emanuel, 2013; Kuang & Hartmann, 2007; Singh & O'Gorman, 2012; Thompson et al., 2017; Zelinka & Hartmann, 2010). Tropical upper tropospheric warming is amplified by a factor of ~2 relative to surface warming (Figure S2c), which means that cloud temperature changes are particularly muted compared to large upper tropospheric warming. Continued research is required to explain the physical mechanisms responsible for the robust and substantial suppression of anvil cloud temperature changes relative to surface warming—behavior that is evident in both models and observations. The rise in high clouds with global warming continues to represent a robust positive feedback.

Our basic finding is that an upward shift of the current distribution of tropical clouds and RH can explain intermodel differences in the simulated response of these fields to CO_2-mediated warming. In the tropics, the magnitude of the vertical shift necessary to explain these hydrologic changes is approximately consistent with the rising isotherms associated with the warming derived from a dilute moist adiabat. To first order, therefore, the simulated distribution of tropical clouds and RH under greenhouse warming can be considered a function of temperature. Since models parameterize cloud behavior (e.g., Geoffroy et al., 2017), it is possible that incorrect parameterizations and/or missing processes (e.g., Jeevanjee et al., 2019) could substantially alter the scaling between the model climatology and response shown here. Fundamentally, however, we have confidence that the depth of the troposphere should increase in response to GHG-driven warming (Santer et al., 2003), and it is reasonable to expect that the current distribution of clouds and water vapor should also show vertical expansion. While it remains to be seen how closely such expansion follows isotherms, evidence from observations (e.g., Zelinka & Hartmann, 2011) and radiative convective equilibrium simulations (Romps, 2014) suggests that such deepening of cloud and water vapor profiles is expected behavior.

Although the predicted-versus-actual changes in tropical upper tropospheric cloud fraction and RH tend to fall along the one-to-one line, the results are noisier at high altitudes for the model cloud lidar data

(Figure 2c). The lidar simulator is intended for direct comparison of model cloud results with observations. We note, however, that some residual artifacts may remain in converting model cloud fields to synthetic lidar fields, particularly for models with lower vertical resolution (e.g., as seen in Figure 2 of Cesana & Chepfer, 2012). It is important to continue to improve the accuracy of both the observations and observational emulators (such as the CALIPSO cloud simulator). Any inaccuracies in the observed or simulated distribution of clouds and RH will affect the apparent constraint shown in Figure 2. Assuming observations are reliable, our results suggest that the intermodel spread in tropical upper tropospheric RH and cloud fraction changes can be reduced by up to 68% if models were to match the observed climatological distribution of clouds and RH.

While the magnitude of the cloud and RH changes is modified by the magnitude of atmospheric warming, the strength of the correlation between the actual and estimated changes in Figure 2 is due entirely to differences in the climatological mean state in CMIP5 models, since the same vertical profile of warming was used in producing the prediction for each model. This is consistent with results from CMIP3 models, in which the vertical gradients in RH scale with the change in RH (Sherwood et al., 2010). In the extratropical upper troposphere, vertical gradients explain a substantial portion of intermodel differences (Figures S6 and S7). This suggests that temperature is an important control on the extratropical distribution of clouds and RH (Thompson et al., 2017), but other processes, such as Hadley Cell expansion, are also important.

The Intergovernmental Panel on Climate Change Fifth Assessment Report concluded that "the range of climate sensitivities and transient responses covered by CMIP3/5 cannot be narrowed significantly by constraining the models with observations of the mean climate and variability" (Flato et al., 2013). Our results show that some aspects of the models' response to GHG forcing are clearly influenced by model representation of the present-day state. This result is in line with other studies that demonstrate a scaling between model climatology and the GHG response of snow albedo (Thackeray et al., 2018), sea ice (Po-Chedley et al., 2018), and clouds (Siler et al., 2018). Such results suggest that biases in the mean state contribute to model spread in the response to GHG forcing. Scientific effort to improve the model representation of cloud and humidity climatologies with respect to observations is clearly warranted.

Acknowledgments
Work performed by Stephen Po-Chedley, Benjamin Santer, and Mark Zelinka at Lawrence Livermore National Laboratory (LLNL) was performed under the auspices of the U.S. Department of Energy under Contract DE-AC52-07NA27344. Initial research by S. P. was supported by the National Science Foundation (AGS-1624881), and subsequent work was carried out under LLNL LDRD 18-ERD-054. Tyler Thorsen was supported by the NASA CALIPSO project. We thank the Gordon Research Conference on Radiation and Climate, which facilitated initial conversations about this research project. We appreciate the helpful suggestions from two anonymous reviewers. We acknowledge the World Climate Research Programme's Working Group on Coupled Modeling, which is responsible for CMIP, and we thank the climate modeling groups for producing and making available their model output (available at https://esgf-node.llnl.gov/search/cmip5/). For CMIP, the U.S. Department of Energy's Program for Climate Model Diagnosis and Intercomparison (PCMDI) provides coordinating support and led development of software infrastructure in partnership with the Global Organization for Earth System Science Portals. ERA5 data were downloaded using the Copernicus Climate Change Service (2019; https://cds.climate.copernicus.eu/); the European Commission nor ECMWF is responsible for any use that may be made of the Copernicus Information or Data it contains. MERRA2 reanalysis data is available online (https://disc.gsfc.nasa.gov/). NASA CALIPSO data were obtained from the NASA Langley Research Center Atmospheric Science Data Center (https://www-calipso.larc.nasa.gov/). AIRS/MLS humidity data can be obtained online (https://catalog.data.gov/dataset/aqua-airs-mls-matchup-indexes-v1-0-airs-mls-ind-at-ges-disc). GOCCP data is available online (https://climserv.ipsl.polytechnique.fr/cfmip-obs/Calipso_goccp.html).

References

Bodas-Salcedo, A., Webb, M. J., Bony, S., Chepfer, H., Dufresne, J.-L., Klein, S. A., et al. (2011). COSP: Satellite simulation software for model assessment. *Bulletin of the American Meteorological Society*, *92*(8), 1023–1043. https://doi.org/10.1175/2011bams2856.1

Caldwell, P. M., Zelinka, M. D., Taylor, K. E., & Marvel, K. (2016). Quantifying the sources of intermodel spread in equilibrium climate sensitivity. *Journal of Climate*, *29*(2), 513–524. Retrieved from http://journals.ametsoc.org/doi/10.1175/JCLI-D-15-0352.1

Cesana, G., & Chepfer, H. (2012). How well do climate models simulate cloud vertical structure? A comparison between CALIPSO-GOCCP satellite observations and CMIP5 models. *Geophysical Research Letters*, *39*, L20803. https://doi.org/10.1029/2012GL053153

Charney, J. G., Arakawa, A., Baker, J. D., Bolin, B., Dickinson, R. E., Goody, R. M., et al. (1979). *Carbon dioxide and climate: A scientific assessment*. Washington, DC: National Academies Press. Retrieved from http://www.nap.edu/catalog/12181, https://doi.org/10.17226/12181

Chepfer, H., Bony, S., Winker, D., Cesana, G., Dufresne, J. L., Minnis, P., et al. (2010). The GCM-oriented CALIPSO Cloud Product (CALIPSO-GOCCP). *Journal of Geophysical Research*, *115*, D00H16. https://doi.org/10.1029/2009JD012251

Chepfer, H., Bony, S., Winker, D., Chiriaco, M., Dufresne, J. L., & Sèze, G. (2008). Use of CALIPSO lidar observations to evaluate the cloudiness simulated by a climate model. *Geophysical Research Letters*, *35*, L15704. https://doi.org/10.1029/2008GL034207

Copernicus Climate Change Service (C3S) (2017). ERA5: Fifth generation of ECMWF atmospheric reanalyses of the global climate from the Copernicus Climate Change Service Climate Data Store (CDS). Retrieved 2019-02-05, from https://cds.climate.copernicus.eu/cdsapp#!/home

Eitzen, Z. A., Xu, K.-M., & Wong, T. (2009). Cloud and radiative characteristics of tropical deep convective systems in extended cloud objects from CERES observations. *Journal of Climate*, *22*(22), 5983–6000. Retrieved from https://doi.org/10.1175/2009JCLI3038.1

Flannaghan, T. J., Fueglistaler, S., Held, I. M., Po-Chedley, S., Wyman, B., & Zhao, M. (2014). Tropical temperature trends in atmospheric general circulation model simulations and the impact of uncertainties in observed SSTs. *Journal of Geophysical Research: Atmospheres*, *119*, 13,327–13,337. https://doi.org/10.1002/2014JD022365

Flato, G., Marotzke, J., Abiodun, B., Braconnot, P., Chou, S. C., Collins, W., et al. (2013). IPCC 2013 AR5—Chapter 9: Evaluation of climate models, *Climate Change 2013: The Physical Science Basis. Contribution of Working Group I to the Fifth Assessment Report of the Intergovernmental Panel on Climate Change* (pp. 741–866). Cambridge, UK: Cambridge University Press. https://doi.org/10.1017/CBO9781107415324

Gelaro, R., McCarty, W., Suárez, M. J., Todling, R., Molod, A., Takacs, L., et al. (2017). The Modern-Era Retrospective Analysis for Research and Applications, Version 2 (MERRA-2). *Journal of Climate*, *30*(14), 5419–5454. Retrieved from https://doi.org/10.1175/JCLI-D-16-0758.1

Geoffroy, O., Sherwood, S. C., & Fuchs, D. (2017). On the role of the stratiform cloud scheme in the inter-model spread of cloud feedback. *Journal of Advances in Modeling Earth Systems*, *9*, 423–437. https://doi.org/10.1002/2016MS000846

Hansen, J., Lacis, A., Rind, D., Russell, G., Stone, P., Fung, I., et al. (1984). Climate sensitivity: Analysis of feedback mechanisms. In J. E. Hansen, & T. Takahashi (Eds.), *Climate processes and climate sensitivity*: American Geophysical Union (AGU). Retrieved from https://agupubs.onlinelibrary.wiley.com/doi/abs/10.1029/GM029p0130

Harrop, B. E., & Hartmann, D. L. (2012). Testing the role of radiation in determining tropical cloud-top temperature. *Journal of Climate*, *25*(17), 5731–5747. https://doi.org/10.1175/JCLI-D-11-00445.1

Hartmann, D. L., Blossey, P. N., & Dygert, B. D. (2019). Convection and climate: What have we learned from simple models and simplified settings?. *Current Climate Change Reports*, *5*, 196–206. Retrieved from http://link.springer.com/10.1007/s40641-019-00136-9

Hartmann, D. L., & Larson, K. (2002). An important constraint on tropical cloud–climate feedback. *Geophysical Research Letters*, *29*(20), 1951. https://doi.org/10.1029/2002GL015835

Held, I. M., & Shell, K. M. (2012). Using relative humidity as a state variable in climate feedback analysis. *Journal of Climate*, *25*(8), 2578–2582. https://doi.org/10.1175/JCLI-D-11-00721.1

Jeevanjee, N., Langhans, W., & Romps, D. M. (2019). Formation of tropical anvil clouds by slow evaporation. *Geophysical Research Letters*, *46*, 492–501. https://doi.org/10.1029/2018GL080747

Jeevanjee, N., & Romps, D. M. (2018). Mean precipitation change from a deepening troposphere. *Proceedings of the National Academy of Sciences*, *115*(45), 11,465–11,470. https://doi.org/10.1073/pnas.1720683115

Jiang, J. H., Su, H., Zhai, C., Wu, L., Minschwaner, K., Molod, A. M., & Tompkins, A. M. (2015). An assessment of upper troposphere and lower stratosphere water vapor in MERRA, MERRA2, and ECMWF reanalyses using Aura MLS observations. *Journal of Geophysical Research: Atmospheres*, *120*, 11,468–11,485. https://doi.org/10.1002/2015JD023752

Khairoutdinov, M., & Emanuel, K. (2013). Rotating radiative-convective equilibrium simulated by a cloud-resolving model. *Journal of Advances in Modeling Earth Systems*, *5*, 816–825. https://doi.org/10.1002/2013ms000253

Kuang, Z., & Hartmann, D. L. (2007). Testing the Fixed Anvil Temperature Hypothesis in a cloud-resolving model. *Journal of Climate*, *20*(10), 2051–2057. https://doi.org/10.1175/JCLI4124.1

Kubar, T. L., Hartmann, D. L., & Wood, R. (2007). Radiative and convective driving of tropical high clouds. *Journal of Climate*, *20*(22), 5510–5526. https://doi.org/10.1175/2007JCLI1628.1

Lau, W. K. M., & Kim, K.-M. (2015). Robust Hadley Circulation changes and increasing global dryness due to CO_2 warming from CMIP5 model projections. *Proceedings of the National Academy of Sciences*, *112*(12), 201418682. https://doi.org/10.1073/pnas.1418682112

Liang, C. K., Eldering, A., Irion, F. W., Read, W. G., Fetzer, E. J., Kahn, B. H., & Liou, K.-N. (2010). Characterization of merged AIRS and MLS water vapor sensitivity through integration of averaging kernels and retrievals. *Atmospheric Measurement Techniques Discussions*, *3*(4), 2833–2859. https://doi.org/10.5194/amtd-3-2833-2010

Lorenz, D. J., & DeWeaver, E. T. (2007). Tropopause height and zonal wind response to global warming in the IPCC scenario integrations. *Journal of Geophysical Research*, *112*, D10119. https://doi.org/10.1029/2006JD008087

Manabe, S., & Wetherald, R. T. (1975). The effects of doubling the CO_2 concentration on the climate of a general circulation model. *Journal of the Atmospheric Sciences*, *32*(1), 3–15. Retrieved from https://doi.org/10.1175/1520-0469(1975)032%3C0003:TEODTC%3E2.0.CO;2, http://journals.ametsoc.org/doi/abs/10.1175/1520-0469%281975%29032%3C0003%3ATEODTC%3E2.0.CO%3B2

Mitchell, J. F. B., & Ingram, W. J. (1992). Carbon dioxide and climate: Mechanisms of changes in cloud. (Vol. 5) (No. 1) https://doi.org/10.1175/1520-0442(1992)005h0005:cdacmoi2.0.co;2

O'Gorman, P. A., & Muller, C. J. (2010). How closely do changes in surface and column water vapor follow Clausius-Clapeyron scaling in climate change simulations? *Environmental Research Letters*, *5*(2), 025207. https://doi.org/10.1088/1748-9326/5/2/025207

Po-Chedley, S., Armour, K. C., Bitz, C. M., Zelinka, M. D., & Santer, B. D. (2018). Sources of intermodel spread in the lapse rate and water vapor feedbacks. *Journal of Climate*, *31*(8), 3187–3206. https://doi.org/10.1175/JCLI-D-17-0674.1

Reichler, T., Dameris, M., & Sausen, R. (2003). Determining the tropopause height from gridded data. *Geophysical Research Letters*, *30*(20), 2042. https://doi.org/10.1029/2003GL018240

Romps, D. M. (2014). An analytical model for tropical relative humidity. *Journal of Climate*, *27*(19), 7432–7449. https://doi.org/10.1175/JCLI-D-14-00255.1

Romps, D. M. (2016). Clausius–Clapeyron scaling of CAPE from analytical solutions to RCE. *Journal of the Atmospheric Sciences*, *73*(9), 3719–3737. Retrieved from http://journals.ametsoc.org/doi/10.1175/JAS-D-15-0327.1

Santer, B. D., Wehner, M. F., Wigley, T. ML, Sausen, R., Meehl, G. A., Taylor, K. E., et al. (2003). Contributions of anthropogenic and natural forcing to recent tropopause height changes. *Science*, *301*(5632), 479–483. https://doi.org/10.1126/science.1084123

Santer, B. D., Wigley, T. M. L., Mears, C., Wentz, F. J., Klein, S. A., Seidel, D. J., et al. (2005). Amplification of surface temperature trends and variability in the tropical atmosphere. *Science (New York, N.Y.)*, *309*(5740), 1551–1556. Retrieved from http://www.sciencemag.org/content/309/5740/1551.abstract

Seeley, J. T., Jeevanjee, N., & Romps, D. M. (2019). FAT or FiTT: Are anvil clouds or the tropopause temperature invariant? *Geophysical Research Letters*, *46*, 1842–1850. Retrieved from https://doi.org/10.1029/2018GL080096

Sherwood, S. C., Ingram, W., Tsushima, Y., Satoh, M., Roberts, M., Vidale, P. L., & O'Gorman, P. A. (2010). Relative humidity changes in a warmer climate. *Journal of Geophysical Research*, *115*, D09104. https://doi.org/10.1029/2009JD012585

Siler, N., Po-Chedley, S., & Bretherton, C. S. (2018). Variability in modeled cloud feedback tied to differences in the climatological spatial pattern of clouds. *Climate Dynamics*, *50*(3-4), 1209–1220. https://doi.org/10.1007/s00382-017-3673-2

Singh, M. S., & O'Gorman, P. A. (2012). Upward shift of the atmospheric general circulation under global warming: Theory and simulations. *Journal of Climate*, *25*(23), 8259–8276. Retrieved from http://journals.ametsoc.org/doi/abs/10.1175/JCLI-D-11-00699.1

Soden, B., & Held, I. (2006). An assessment of climate feedbacks in coupled ocean–atmosphere models. *Journal of Climate*, *19*(2003), 3354–3360. Retrieved from http://www.gfdl.noaa.gov/bibliography/related_files/bjs0601.pdf

Taylor, K. E., Stouffer, R. J., & Meehl, G. A. (2012). An overview of CMIP5 and the experiment design. *Bulletin of the American Meteorological Society*, *93*(4), 485–498. Retrieved from http://journals.ametsoc.org/doi/abs/10.1175/BAMS-D-11-00094.1

Thackeray, C. W., Qu, X., & Hall, A. (2018). Why do models produce spread in snow albedo feedback?. *Geophysical Research Letters*, *45*, 6223–6231. https://doi.org/10.1029/2018GL078493

Thompson, D. W. J., Bony, S., & Li, Y. (2017). Thermodynamic constraint on the depth of the global tropospheric circulation. *Proceedings of the National Academy of Sciences*, *114*(31), 8181–8186. https://doi.org/10.1073/pnas.1620493114

Thompson, D. W. J., Ceppi, P., & Li, Y. (2019). A robust constraint on the temperature and height of the extratropical tropopause. *Journal of Climate*, *32*(2), 273–287. https://doi.org/10.1175/JCLI-D-18-0339.1

Vial, J., Dufresne, J.-L., & Bony, S. (2013). On the interpretation of inter-model spread in CMIP5 climate sensitivity estimates. *Climate Dynamics*, *41*(11-12), 3339–3362. Retrieved from http://link.springer.com/10.1007/s00382-013-1725-9

Wetherald, R. T., & Manabe, S. (1980). Cloud cover and climate sensitivity. *Journal of the Atmospheric Sciences*, *37*(7), 1485–1510. Retrieved from http://journals.ametsoc.org/doi/abs/10.1175/1520-0469%281980%29037%3C1485%3ACCACS%3E2.0.CO%3B2

Winker, D. M., Vaughan, M. A., Omar, A., Hu, Y., Powell, K. A., Liu, Z., et al. (2009). Overview of the CALIPSO mission and CALIOP data processing algorithms. *Journal of Atmospheric and Oceanic Technology*, *26*(11), 2310–2323. Retrieved from http://journals.ametsoc.org/doi/abs/10.1175/2009JTECHA1281.1

Xu, K.-M., Wong, T., Wielicki, B. A., Parker, L., Lin, B., Eitzen, Z. A., & Branson, M. (2007). Statistical analyses of satellite cloud object data from CERES. Part II: Tropical convective cloud objects during 1998 El Niño and evidence for supporting the Fixed Anvil Temperature Hypothesis. *Journal of Climate*, *20*(5), 819–842. Retrieved from https://doi.org/10.1175/JCLI4069.1

Zelinka, M. D., & Hartmann, D. L. (2010). Why is longwave cloud feedback positive? *Journal of Geophysical Research*, *115*, D16117. https://doi.org/10.1029/2010JD013817

Zelinka, M. D., & Hartmann, D. L. (2011). The observed sensitivity of high clouds to mean surface temperature anomalies in the tropics. *Journal of Geophysical Research*, *116*, D23103. https://doi.org/10.1029/2011JD016459

Zelinka, M. D., Zhou, C., & Klein, S. A. (2016). Insights from a refined decomposition of cloud feedbacks. *Geophysical Research Letters*, *43*, 9259–9269. https://doi.org/10.1002/2016GL069917